

# A Lysosome-Targetable and Two-Photon Fluorescent Probe for Monitoring Endogenous and Exogenous Nitric Oxide in Living Cells

Haibo Yu,<sup>†</sup> Yi Xiao,<sup>\*,†</sup> and Liji Jin<sup>\*,‡</sup>

<sup>†</sup>State Key Laboratory of Fine Chemicals and <sup>‡</sup>School of Life Science and Technology, Dalian University of Technology, Dalian 116024, China

## Supporting Information

**ABSTRACT:** A lysosome-specific and two-photon fluorescent probe, **Lyso-NINO**, demonstrates high selectivity and sensitivity toward NO, lower cytotoxicity, and perfect lysosomal localization. With the aid of **Lyso-NINO**, the first capture of NO within lysosomes of macrophage cells has been achieved using both two-photon fluorescence microscopy and flow cytometry.

Recently, it has been discovered that lysosomal functions are subtly regulated by nitric oxide (NO), a ubiquitous cellular messenger molecule in the cardiovascular, nervous, and immune systems.<sup>1</sup> NO exhibits complex effects on the catabolic autophagy process,<sup>2</sup> which involves the degradation of a cell's own components through the lysosomal machinery, to supply energy and nutrient sources for cell growth,<sup>3</sup> and is also closely related to various disorders and diseases including lysosomal storage disorders,<sup>4</sup> Gaucher's disease,<sup>5</sup> and Danon disease.<sup>6</sup> Endogenous NO, induced by some stimulants including Lipopolysaccharide (LPS) and Interferon- $\gamma$  (IFN- $\gamma$ ), has been reported to react with several related proteins outside lysosomes to drive the autolysosome process by releasing the upstream signals.<sup>7</sup> However, the effects of NO on lysosomes are far from being completely understood. Owing to the dynamic transformation of the morphology and components of the highly heterogeneous lysosomes, it is difficult to find solid evidence of direct interactions between NO and components within lysosomes, but that does not mean they are non-existent. So far, scientists have no tool to determine whether NO enters into lysosomes, not to mention its quantification.

To our knowledge, fluorescent probes—powerful tools in cell biology—can hardly meet the requirements for monitoring lysosomal NO. A variety of NO-sensitive fluorescent molecular probes have already been developed to image intracellular NO under one-photon microscopy (OPM),<sup>8</sup> which has significantly enriched our knowledge about NO homeostasis and NO's critical roles in many biological processes.<sup>9</sup> Nevertheless, none of these probes is well suited for lysosomal applications; they all failed to specifically localize in lysosomes and monitor lysosomal NO.

Besides the lack of lysosomal specificity, another disadvantage of the known NO probes is the lower two-photon fluorescence activity, which gives them poor applicability in two-photon microscopy (TPM). The TPM technique, exciting the fluorophores with NIR laser pulses, has become a potent alternative to OPM because it overcomes latter's problems of

shallow penetration depth, photodamage, and cellular autofluorescence.<sup>10</sup>

Herein, based on the principle of photoinduced electron transfer (PET), a lysosome-targeted and two-photon NO fluorescent probe, **Lyso-NINO**, has been designed through integration of NO-capturing *o*-phenylenediamine, lysosome-targeting (aminoethyl)morpholine, and efficient two-photon fluorophore naphthalimide, as shown in Scheme 1. *o*-Phenyl-

**Scheme 1. Chemical Structure of Lyso-NINO and the Reaction of Lyso-NINO with NO**



enediamine, employed not only as an electron donor (a fluorescence quencher) for naphthalimide but also as a NO trapper, was directly tethered to the imide position of naphthalimide. Accordingly, the 4 position of naphthalimide could be preserved and further modified with 4-(2-aminoethyl)morpholine. The alkylmorpholine group, possessing a lower  $pK_a$  value, targets lysosomes that contain a lot of acid hydrolases in the pH range from 4.5 to 5.5.<sup>11,12</sup>

First, our study on **Lyso-NINO** and **Lyso-NINO-T**'s pH responses confirms the probe's suitability to lysosomal pH range. As shown in Figure 1, the  $pK_a$  of **Lyso-NINO-T** is  $5.61 \pm 0.02$ , which is in good accord with the  $pK_a$  value of the well-known LysoSensor DND-189 ( $pK_a = 5.80$ ).<sup>12</sup> This should be attributed to the lower pH response of the morpholine group. Compared with **Lyso-NINO-T**, **Lyso-NINO** has a lower  $pK_a$  value,  $3.47 \pm 0.01$ , which is ascribed to the pH independence of *o*-phenylenediamine. From these results, we could predict that, in lysosomal pH ranges such as pH 4.5–5.5, there would be very weak fluorescence for **Lyso-NINO**, yet **Lyso-NINO-T** would exhibit a strong fluorescence at the same pH value.

**Lyso-NINO** exhibits high selectivity for NO over other reactive oxygen species and high sensitivity, with a nanomolar-scale limit of detection. **Lyso-NINO** in free form displays a

Received: September 10, 2012

Published: October 8, 2012

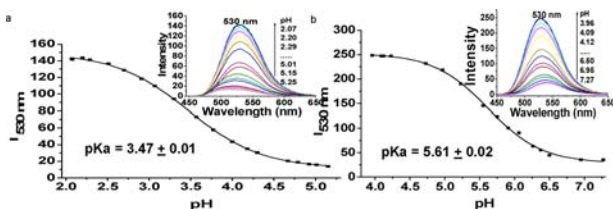


**Figure 1.** Change of intensity plots of (a) Lyso-NINO (11 μM) and (b) Lyso-NINO-T (25 μM) at 530 nm vs different pH values. Inset: change in fluorescence spectra of Lyso-NINO and Lyso-NINO-T in aqueous solution containing 20% acetonitrile as cosolvent vs different pH values ( $\lambda_{\text{ex}} = 440$  nm; slit = 3 nm).

broad absorption band centered at 430 nm ( $\epsilon = 14\,500\text{ M}^{-1}\text{ cm}^{-1}$ ) with almost no fluorescence (fluorescence quantum yield  $\Phi = 0.02$ ) in aqueous buffer at pH 5.0. In the presence of 5.0 equiv of NO solution, the emission spectrum of Lyso-NINO exhibited a remarkable enhancement (16 times) at 530 nm (Figure S2), and the fluorescence quantum yield increased from 0.02 to 0.3. However, the presence of various reactive oxygen and reactive nitrogen species, such as  $\text{H}_2\text{O}_2$ ,  $\text{NO}_2^-$ ,  $\text{NO}_3^-$ ,  $^1\text{O}_2$ ,  $^{\bullet}\text{OH}$ , and  $\text{ONOO}^-$  (Figure 2a), does not cause an observable

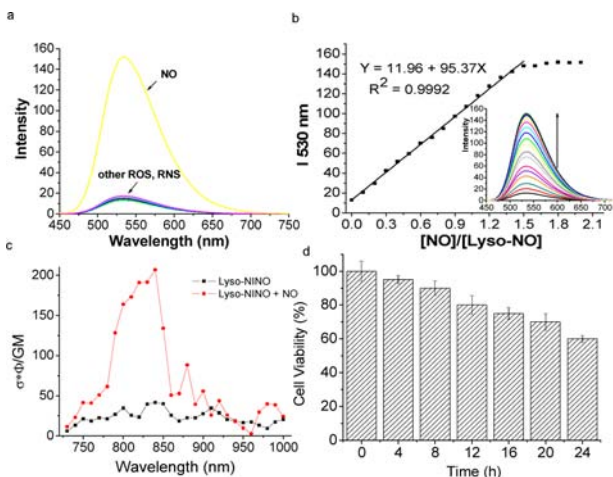


**Figure 2.** (a) Selectivity of Lyso-NINO (11 μM) fluorescence response for NO over other reactive nitrogen and oxygen species (5.0 equiv) in 20:80 CH<sub>3</sub>CN–H<sub>2</sub>O solution at pH 5.0 (in 10 mM phosphate buffer). (b) Intensity at 530 nm vs NO concentration under the same conditions. Inset: changes in fluorescence spectra of Lyso-NINO (11 μM) upon addition of different amounts NO solution (0–2.0 equiv). (c) Two-photon action spectra of Lyso-NINO (in phosphate buffer pH 5.0) before (black) and after (red) addition of NO solution (5.0 equiv). (d) Cell viability of Lyso-NINO (5.0 μM) at different times.

spectral change. The titrations of Lyso-NINO with NO are examined in a mixture of acetonitrile and sodium phosphate buffer. Upon addition of NO solution, a new emission peak at 530 nm increases gradually (Figure 2b); meanwhile, the absorption spectra do not change during the titration of NO (Figure S3), which indicates that nitric oxide reacts with *o*-phenylenediamine moiety, a result of inhibition of the PET process from the *o*-phenylenediamine moiety to the naphthalimide fluorophore. The *in situ*-formed NO product of Lyso-NINO without any byproduct, as expected, is confirmed to be Lyso-NINO-T, according to retention times and typical HPLC absorption spectra (Figure S4). With increasing of NO, an excellent linear correlation ( $R^2 = 0.9992$ ) between fluorescence

intensity (530 nm) and NO concentration is found in the range of NO concentration from 1 to 1.3 μM (Figure 2b). The limit of detection ( $S/N = 3$ ) of Lyso-NINO is determined to be 5 nM (Supporting Information), indicating that Lyso-NINO would be a potential tool to monitor endogenous NO in live cells.

Lyso-NINO displays significant applicability under two-photon excitation. The maximum two-photon action cross-section ( $\Phi\delta$ ) value is 34 GM at 840 nm.<sup>13</sup> Upon addition of NO solution (5.0 equiv), the maximum two-photon action cross section increases to 210 GM at 840 nm (Figure 2c). Such a drastic enhancement in two-photon excitation fluorescence indicates that Lyso-NINO is a potential two-photon probe for monitoring and imaging NO in living specimens.

The cytotoxicity of Lyso-NINO is low in the first 12 h of incubation. MTT assay (SI) has revealed that 80% of MCF-7 cells survive after incubation with Lyso-NINO (5.0 μM) for 12 h, and 24 h later the survival rate is over 60% (Figure 2d). As is well known, most lysosomal probes bearing basic groups exhibit an alkalinizing effect on the lysosomes, such that longer incubation with these probes can induce an increase in lysosomal pH and result in cell death. Although there is significant cell death within 24 h incubation time, in the first 12 h the survival rate of these cells incubated with Lyso-NINO is high: up to 80%. Compared with some commercial lysosomal probes, the lower cytotoxic effect of Lyso-NINO on MCF-7 cells is a favorable characteristic of a practical NO probe for application in living cells.

Lyso-NINO exhibits a significant ability to target lysosomes. Co-localization experiments are performed by co-staining MCF-7 cells with Neutral Red (NR), a commercial LysoTracker, and tetramethylrhodamine methyl (TMRM), a mitochondria tracker. MCF-7 cells stained with Lyso-NINO for 10 min at 37 °C do not show green fluorescence in Channel 1 (Figure S5); after that, in the presence of 5.0 equiv of NO solution, these cells display measurable levels of green TP fluorescence in discrete subcellular locations (Figure 3a). The TPM image merges well with the image of staining with NR (Figure 3c) rather than TMRM (Figure S6), indicating that Lyso-NINO can specifically localize in lysosomes rather than mitochondria of living cells. The intensity profiles of the linear regions of interest across MCF-7 cells stained with Lyso-NINO and NR also vary in close synchrony (Figure 3d). The high Pearson's coefficient and overlap coefficient are 0.805 and 1.374, respectively, evaluated using the conventional dye-overlay method (Figure S7).

Lyso-NINO and NR display a good coexistence in lysosomes of MCF-7 cells, yet the differences in fluorescence intensity between the two channels, which may provide more useful information about the internal environment of organelles in living cells, should be noted. Thus, an intensity correlation analysis (ICA)<sup>14</sup> is employed to assess the intensity distribution of the two co-existing dyes. We plot the intensity of stain Lyso-NINO against that of NR for each pixel. The dependent staining in Figure 3c results in a highly correlated plot (Figure 3e), and the ICA plots for the two stains generate an unsymmetrical hourglass-shaped scatterplot that is markedly skewed toward positive values (Figure 3f,g). Moreover, the intensity correlation quotient (ICQ) for the two dyes is 0.357, very close to 0.5, suggesting that the staining intensities are dependent on each other. From the product of the differences from the mean (PDM) image with positive values in the pixels (Figure 3h), we can easily identify those lysosomes with high

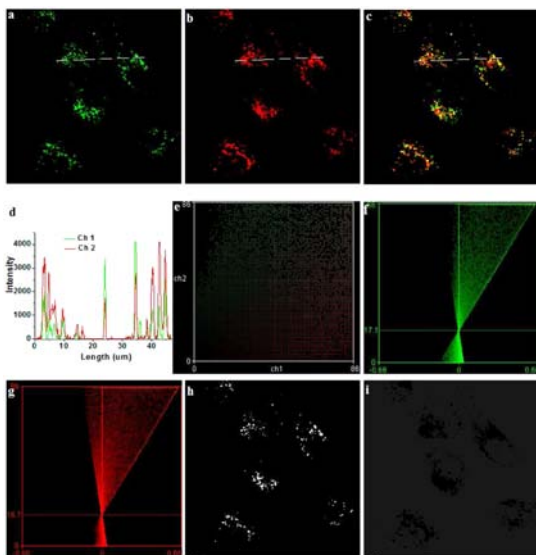


**Figure 3.** Lyso-NINO co-localizes to lysosomes in MCF-7 cells. MCF-7 was stained with (a) 5.0  $\mu\text{M}$  Lyso-NINO with NO solution (20  $\mu\text{M}$ ) for 5 min at 37  $^{\circ}\text{C}$  (Channel 1:  $\lambda_{\text{ex}} = 840 \text{ nm}$ ,  $\lambda_{\text{em}} = 520\text{--}560 \text{ nm}$ ) and (b) 5.0  $\mu\text{M}$  NR (Channel 2:  $\lambda_{\text{ex}} = 559 \text{ nm}$ ,  $\lambda_{\text{em}} = 565\text{--}610 \text{ nm}$ ). (c) Overlay of (a) and (b). (d) Intensity profile of regions of interest (ROI) across MCF-7 cells. (e) Intensity correlation plot of stain Lyso-NINO and NR. ICA plots of (f) stain Lyso-NINO, and (g) stain NR. PDM images with (h) positive PDM values in the pixels and (i) negative PDM values in the pixels.

intensity distribution of the two dyes (white pixels in Figure 3h). There are also some lysosomes for which the intensity distribution does not vary synchronously (Figure 3i). The reason might be that nitrite ions, byproducts of NO, react with NR in acidic conditions and deplete the fluorescence intensity of NR in some lysosomes.<sup>15</sup> On the other hand, the PDM image with negative values in the pixels (Figure 3i) further demonstrates that Lyso-NINO is a lysosome-specific probe for NO and the byproduct of NO in lysosomes does not interfere with its photoproperties.

Owing to its high selectivity and sensitivity, Lyso-NINO is used as a fluorescent indicator to assess exogenous and endogenous NO in living cells. In view of NO releaser widely used in the treatment of cancer,<sup>16</sup> herein, we employ Lyso-NINO to monitor the releasing process of NO from NOC13 in lysosomes of MCF-7 cells. NOC13 (5.0 equiv) is added into MCF-7 cells incubated with Lyso-NINO, and the fluorescence intensity gradually increases over time and reaches the maximum after 15 min (Figure 4a). The gradually increasing intensity in lysosomes demonstrates that NO releasing from NOC13 is able to diffuse into lysosomes and then be captured by lysosomes-targeting Lyso-NINO. The efficacy of Lyso-NINO for endogenous NO is also investigated. Macrophages RAW264.7 incubated with Lyso-NINO for 12 h at 37  $^{\circ}\text{C}$  display a weak fluorescence (Figure 4b), which indicates that Lyso-NINO could capture endogenous NO in lysosomes of macrophages. Stimulation with L-arginine (L-Arg), interferon- $\gamma$  (IFN- $\gamma$ ), and Lipopolysaccharide (LPS) in the presence of Lyso-NINO has led to a pronounced increase in fluorescence intensity (Figure 4c), indicating that, despite the shorter lifetime of NO, endogenous NO may easily diffuse into lysosomes in living cells.

Lyso-NINO also shows good applicability in flow cytometry (FCM). FCM can be used to quantitatively evaluate

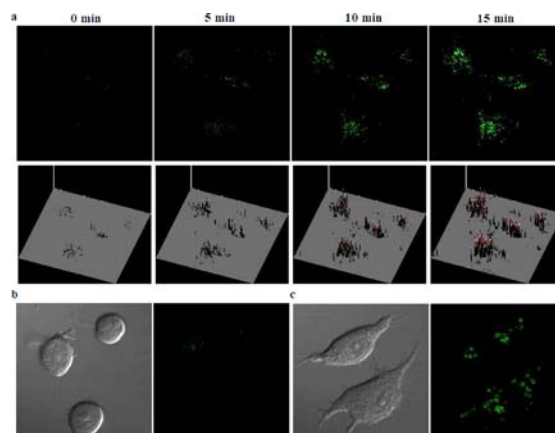


**Figure 4.** (a) Time-dependent exogenous NO released from NOC13 (20  $\mu\text{M}$ ) in MCF-7 cells stained with Lyso-NINO (5.0  $\mu\text{M}$ ). (b) DIC image and two-photon fluorescent image of RAW 264.7 macrophages stained with Lyso-NINO (5.0  $\mu\text{M}$ ) for 4 h at 37  $^{\circ}\text{C}$ . (c) DIC image and two-photon fluorescent image of RAW 264.7 macrophages co-stained with Lyso-NINO (5.0  $\mu\text{M}$ ) and stimulants containing final concentrations of 5000  $\mu\text{g}/\text{mL}$  L-Arg, 150 units/mL IFN- $\gamma$ , and 20  $\mu\text{g}/\text{mL}$  LPS for 12 h,  $\lambda_{\text{ex}} = 840 \text{ nm}$ ,  $\lambda_{\text{em}} = 520\text{--}560 \text{ nm}$ .

endogenous NO in individual cells on a large scale, compared with microscopy imaging which provides spatial information. Histograms demonstrate intracellular accumulation of NO and increase of intracellular fluorescence indicated by the shift of the fluorescence signal measured in the FITC channel (Figure 5). Compared with control cells without staining (Figure

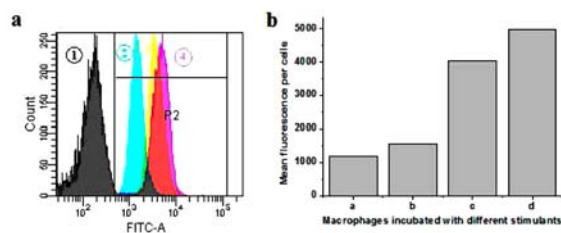


**Figure 5.** (a) Flow cytometric analysis of Macrophages loaded with Lyso-NINO and different stimulants. (1) Control group: Macrophages loaded without Lyso-NINO. (2) Macrophages loaded with Lyso-NINO (5.0  $\mu\text{M}$ ) for 12 h at 37  $^{\circ}\text{C}$ . (3) Macrophages loaded with Lyso-NINO (5.0  $\mu\text{M}$ ), L-Arg(5000  $\mu\text{g}/\text{mL}$ ), and LPS (20  $\mu\text{g}/\text{mL}$ ) for 12 h 37  $^{\circ}\text{C}$ . (4) Macrophages co-incubated with Lyso-NINO (5.0  $\mu\text{M}$ ), L-Arg(5000  $\mu\text{g}/\text{mL}$ ), IFN- $\gamma$  (150 units/mL), and LPS (20  $\mu\text{g}/\text{mL}$ ) for 12 h 37  $^{\circ}\text{C}$ . (b) Mean fluorescence per macrophage cell of (1), (2), (3), and (4) incubation conditions.

5a(1)), macrophages incubated only with Lyso-NINO for 12 h show a significant fluorescence from the histogram (Figure 5a(2)). Incubation of cells with Lyso-NINO, L-Arg, and LPS for 12 h shifts the histogram of green fluorescence in the direction of higher intensity (Figure 5a(3)). However, in the absence and presence of IFN- $\gamma$ , the histograms of fluorescence intensity do not shift much higher (Figure 5a(4)). Quantification by mean fluorescence of these macrophages (Figure 5b) suggests that LPS would be a critical factor which effectively induces an increase of endogenous NO in live macrophages.

In this paper, there are two significant aspects: (1) A lysosomal-specific and two-photon fluorescent probe Lyso-NINO has been first developed, and it demonstrates high selectivity and sensitivity toward NO over other reactive oxygen

and nitrogen species, lower cytotoxicity than commercial lysosomal probes, and perfect lysosomal localization. (2) For the first time, endogenous NO has been captured in lysosomes of macrophage cells, despite the unknown NO source. We anticipate that these results would inspire and encourage lots of researchers to focus on the regulation effects of NO on lysosomes in the biology and pharmacology.

## ■ ASSOCIATED CONTENT

### 📄 Supporting Information

Synthesis, characterization, and experimental details. This material is available free of charge via the Internet at <http://pubs.acs.org>.

## ■ AUTHOR INFORMATION

### Corresponding Author

xiaoyi@dlut.edu.cn; jinlijij@dlut.edu.cn

### Notes

The authors declare no competing financial interest.

## ■ ACKNOWLEDGMENTS

This work was supported by National Natural Science Foundation of China (No. 21174022), National Basic Research Program of China (No. 2013CB733702), and Specialized Research Fund for the Doctoral Program of Higher Education (No. 20110041110009).

## ■ REFERENCES

- (1) (a) Snyder, S. H. *Science* **1992**, *257*, 494–496. (b) Klionsky, D. J.; Emr, S. D. *Science* **2000**, *290*, 1717–1721. (c) Shintani, T.; Klionsky, D. J. *Science* **2004**, *306*, 990–995.
- (2) Sarkar, S.; Korolchuk, V. I.; Renna, M.; Imarisio, S.; Fleming, A.; Williams, A.; Garcia-Arencibia, M.; Rose, C.; Luo, S. Q.; Underwood, B. R.; Kroemer, G.; O’Kane, C. J.; Rubinsztein, D. C. *Mol. Cell* **2011**, *43*, 19–32.
- (3) (a) Rabinowitz, J. D.; White, E. *Science* **2010**, *330*, 1344–1348. (b) Xie, Z. P.; Klionsky, D. J. *Nat. Cell Biol.* **2007**, *9*, 1102–1109.
- (4) Ballabio, A.; Gieselmann, V. *BBA-Mol. Cell Res.* **2009**, *1793*, 684–696.
- (5) (a) Cox, T. M. *J. Inherit. Metab. Dis.* **2001**, *24*, 106–121. (b) Aerts, J. M. F. G.; Hollak, C. E. M. *Bailliere Clin. Haem.* **1997**, *10*, 691–709. (c) Pavlova, E. V.; Deegan, P. B.; Tindall, J.; McFarlane, I.; Mehta, A.; Hughes, D.; Wraith, J. E.; Cox, T. M. *Blood Cell Mol. Dis.* **2011**, *46*, 27–33.
- (6) (a) Holton, J. L.; Beesley, C.; Jackson, M.; Venner, K.; Bhardwaj, N.; Winchester, B.; Al-Memmar, A. *Neuropath. Appl. Neuro.* **2006**, *32*, 253–259. (b) Levine, B.; Klionsky, D. J. *Dev. Cell* **2004**, *6*, 463–477. (c) Stromhaug, P. E.; Klionsky, D. J. *Traffic* **2001**, *2*, 524–531.
- (7) (a) Yuan, H.; Perry, C. N.; Huang, C. Q.; Iwai-Kanai, E.; Carreira, R. S.; Glembofski, C. C.; Gottlieb, R. A. *Am. J. Physiol.-Heart C* **2009**, *296*, 470–479. (b) da Silva, T. R. M.; de Freitas, J. R.; Silva, Q. C.; Figueira, C. P.; Roxo, E.; Leao, S. C.; de Freitas, L. A. R.; Veras, P. S. T. *Infect. Immun.* **2002**, *70*, 5628–5634.
- (8) (a) Kojima, H.; Nakatsubo, N.; Kikuchi, K.; Kawahara, S.; Kirino, Y.; Nagoshi, H.; Hirata, Y.; Nagano, T. *Anal. Chem.* **1998**, *70*, 2446–2453. (b) Pluth, M. D.; McQuade, L. E.; Lippard, S. J. *Org. Lett.* **2010**, *12*, 2318–2321. (c) Pluth, M. D.; Chan, M. R.; McQuade, L. E.; Lippard, S. J. *Inorg. Chem.* **2011**, *50*, 9385–9392. (d) Yuan, L.; Lin, W. Y.; Xie, Y. N.; Chen, B.; Song, J. Z. *Chem. Commun.* **2011**, *47*, 9372–9374. (e) Hu, X. Y.; Wang, J.; Zhu, X.; Dong, D. P.; Zhang, X. L.; Wu, S. O.; Duan, C. Y. *Chem. Commun.* **2011**, *47*, 11507–11509. (f) Lin, L. Y.; Lin, X. Y.; Lin, F.; Wong, K. T. *Org. Lett.* **2011**, *13*, 2216–2219. (g) Chen, Y. G.; Guo, W. H.; Ye, Z. Q.; Wang, G. L.; Yuan, J. L. *Chem. Commun.* **2011**, *47*, 6266–6268. (h) Yang, Y. J.; Seidlits, S. K.; Adams, M. M.; Lynch, V. M.; Schmidt, C. E.; Anslyn, E. V.; Shear, J. B. *J. Am. Chem. Soc.* **2010**, *132*, 13114–13116.

- (9) (a) Sasaki, E.; Kojima, H.; Nishimatsu, H.; Urano, Y.; Kikuchi, K.; Hirata, Y.; Nagano, T. *J. Am. Chem. Soc.* **2005**, *127*, 3684–3685. (b) Tonzetich, Z. J.; McQuade, L. E.; Lippard, S. J. *Inorg. Chem.* **2010**, *49*, 6338–6348.
- (10) (a) Lim, C. S.; Masanta, G.; Kim, H. J.; Han, J. H.; Kim, H. M.; Cho, B. R. *J. Am. Chem. Soc.* **2011**, *133*, 11132–11135. (b) Pawliki, M.; Collins, H. A.; Denning, R. G.; Anderson, H. L. *Angew. Chem., Int. Ed.* **2009**, *48*, 3244–3266. (c) He, G. S.; Tan, L. S.; Zheng, Q.; Prasad, P. N. *Chem. Rev.* **2008**, *108*, 1245–1330. (d) Denk, W.; Strickler, J. H.; Webb, W. W. *Science* **1990**, *248*, 73–76.
- (11) Rink, T. J.; Tsien, R. Y.; Pozzan, T. *J. Cell Biol.* **1982**, *95*, 189–196.
- (12) de Silva, A. P.; Gunaratne, H. Q. N.; Lynch, P. L. M.; Patty, A. J.; Spence, G. L. *J. Chem. Soc., Perkin Trans. 2* **1993**, 1611–1616.
- (13) (a) Xu, C.; Webb, W. W. *J. Opt. Soc. Am. B* **1996**, *13*, 481–491. (b) Lee, S. K.; Yang, W. J.; Choi, J. J.; Kim, C. H.; Jeon, S.-J.; Cho, B. R. *Org. Lett.* **2005**, *7*, 323–326.
- (14) Li, Q.; Lau, A.; Morris, T. J.; Guo, L.; Fordyce, C. B.; Stanley, E. F. *J. Neurosci.* **2004**, *24*, 4070–4081.
- (15) Afkhami, A.; Mogharnesband, A. A. *Anal. Lett.* **1994**, *27*, 991–1000.
- (16) (a) Safdar, S.; Taite, L. J. *Int. J. Pharm.* **2012**, *422*, 264–270. (b) Lu, Y.; Sun, B.; Li, C. H.; Schoenfisch, M. H. *Chem. Mater.* **2011**, *23*, 4227–4233. (c) Chakrapani, H.; Wilde, T. C.; Citro, M. L.; Goodblatt, M. M.; Keefer, L. K.; Saavedra, J. E. *Bioorg. Med. Chem.* **2008**, *16*, 2657–2664.